

RECONSTRUCTION OF α -IRON $\langle 100 \rangle$ SYMMETRIC TILT GRAIN BOUNDARIES $\Sigma 17(410)$ AND $\Sigma 13(510)$

Eva Vitková — Peter Ballo *

A detailed numerical study on structure of symmetric tilt grain boundaries in α -iron is presented. The study is focused on structural and energetic optimization of $\langle 100 \rangle$ grain boundaries $\Sigma 5(210)$, $\Sigma 5(310)$, $\Sigma 17(410)$ and $\Sigma 13(510)$. Particular attention is given to grain boundary reconstruction, which is characterized by increased atomic density in grain boundary plane compared to bulk. The results of our numerical experiments significantly improved our knowledge about the migration of atoms between planes perpendicular as well as parallel to GB plane as an essential part of grain boundary reconstruction.

Key words: iron, grain boundary, relaxation, reconstruction, structural optimization, atomic migration

1 INTRODUCTION

Ferritic steel is one of the most promising structural materials for new generation of fusion and fission reactors [1–3]. Key factor of these materials, which is in fact bcc-iron (α -iron) in polycrystalline form, is structural stability concerning high safety and long operating life of the reactors. While the base material is in polycrystalline form, grain boundary (GB) as an interface between two grains plays crucial role in material stability. Close to GB the spatial arrangement of lattice planes, their crystallographic structure as well as dynamics of the constituent atoms may differ from the corresponding features in the grain. From microscopical point of view, the crystal structure along the GBs is mainly responsible for changes in physical properties of polycrystalline as well as nanocrystalline materials [4–6]. Consequently, a detailed understanding of the mechanism of formation and development of GBs is an important step in the creation of new structural materials with well-defined parameters and long time stability.

The most common method used to describe high-angle grain boundary structure is Coincidence Site Lattice (CSL) theory. However, geometrical models constructed according this theory are idealized, far from equilibrium, and therefore additional atomic optimization is essential. Different geometry and force field acting on surface or interface atoms cause change in in-plane and also inter-planar atomic arrangement. The level of optimization can be described from energetics point of view by GB energy or from geometrical point of view by terms relaxation and reconstruction. Low GB energy indicates stable interface. When the change of symmetry or topology of interface plane occurs we talk about reconstruction, otherwise it is relaxation. Typical relaxation, except small distortion of in-plane crystalline structure, is also change of inter-planar distances parallel to interface [7].

It should be noted that there are some discrepancies in obtained α -iron GB energies [8,9]. For example, the difference between GB $\Sigma 13(510)$ energies presented in works [8] and [9] is almost 1 Jm^{-2} . The discrepancies can be caused by different description of atomic interaction, which is not the case here. We will show that discrepancy in obtained energies is consequence of applied optimization techniques reaching different local minima corresponding to relaxed and reconstructed GB structures.

The aim of this work is detailed structural study of α -iron $\langle 100 \rangle$ symmetric tilt GBs on atomic scale level. We will focus on GBs $\Sigma 5(210)$, $\Sigma 5(310)$, $\Sigma 17(410)$ and $\Sigma 13(510)$. The article is arranged as follows: GB supercell construction, atomic interaction and optimization method is described in Sec. 2. In Sec. 3 the main result, detailed description of the reconstruction process of GBs $\Sigma 17(410)$ and $\Sigma 13(510)$, is presented and finally the main contribution of our work is summarized in Sec. 4.

2 THEORETICAL PART

Initial grain boundary models were constructed according to CSL theory. Two bcc-grains were rotated towards each other around the $[001]$ rotation axis and then matched together. This geometry in combination with periodical boundary conditions creates computational cell, which contains two GBs. First of them is positioned in the middle of the computational cell (GB1) while second one (GB2) is from geometrical reasons split into two parts positioned on the top and bottom edge of the cell. Computational cell we will refer as supercell. Initial geometrical models of computational supercells are shown in Fig. 1 and information about dimensions, number of atoms and misorientation angle of used supercells are summarized in Table 1. Note, the dimensions of supercells in z -direction were chosen to be large enough to exclude interactions

* Slovak University of Technology in Bratislava, Ilkovičova 3, 812 19 Bratislava 1, Slovakia, atavaha@hotmail.com peter.ballo@stuba.sk

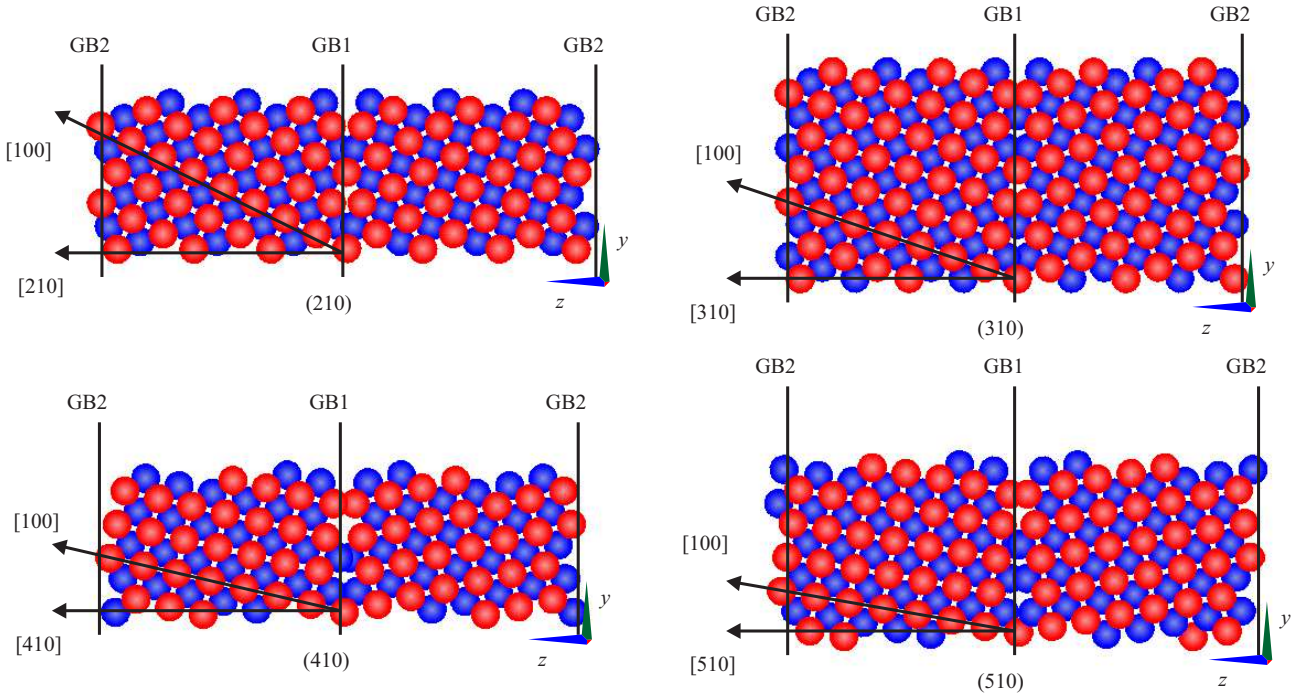


Fig. 1. Models of α -iron $\langle 100 \rangle$ symmetric tilt grain boundaries (a) — $\Sigma 5(210)$, (b) — $\Sigma 5(310)$, (c) — $\Sigma 17(410)$, (d) — $\Sigma 13(510)$. Red and blue color represents atoms placed in planes (001) and (002), respectively.

Table 1. Parameters of α -iron $\langle 100 \rangle$ symmetric tilt grain boundary simulation supercells: misorientation angle (α), dimensions in x -, y -, z -direction (sx , sy , sz), number of atoms (nat)

GB	α ($^\circ$)	sx (\AA)	sy (\AA)	sz (\AA)	nat
$\Sigma 5(210)$	53.13	14.275	12.768	40.857	640
$\Sigma 5(310)$	36.87	17.130	18.057	37.919	1008
$\Sigma 17(410)$	28.072	11.420	11.772	38.777	448
$\Sigma 13(510)$	22.62	14.275	14.558	39.194	700

between GBs positioned in the middle and edge of supercells.

Before the optimization process, the supercells were divided into two parts: one part where atoms fulfil condition $|z| \leq sz/4$ and the second one where atoms fulfil complementary condition $|z| > sz/4$. Note, z is atomic coordinate in z -direction, sz is supercell dimension in z -direction, and GB plane is situated at position $z = 0$. The first part including GB1 (see Fig. 1) was optimized by combination of simulated annealing and genetic algorithm optimization methods. Grain boundary GB2 positioned at the edge of the supercell remained in its initial geometrical configuration.

A very important parameter that is used for the assessment of the optimization result is an energy of GB, which is defined as

$$E_{GB} = \frac{2E_2 - E_1 - NE_c}{2sxsy}, \quad (1)$$

where E_2 is energy of supercell with one unoptimized and one optimized GB, E_1 is energy of supercell with two

unoptimized GBs, N is number of atoms in supercell, E_c is cohesive energy and $sxsy$ is GB area.

Atomic interaction at microscopic level was described by Embedded-Atom Method (EAM) [10] potential, which was originally developed for fcc metals. Later it was parametrized even for bcc metals. In our experiments, we used parametrization provided by Mendevlev *et al* [11]. According to this parametrization, a lattice parameter for α -iron was set up to 2.855 \AA . It is a widely accepted fact that the quality of the results depends on the quality of individual features used in the the EAM equation. Using the same functions we should get the same result. However, we must not forget the impact of the optimization process that typically influences the result. Periodical boundary conditions were realized by minimum image convention method. That is why the supercell dimensions have to obey condition

$$r_{\text{cutoff}} \leq 0.5L, \quad (2)$$

where r_{cutoff} is cutoff radius defined by EAM potential and L is arbitrary supercell dimension.

Another important parameter we will use to describe the interface is the width of GB (w). The parameter quantifies how far the effect of relaxation caused by a core of GB extends towards the bulk. For our purposes, we set the width of GB as an area where the average energy of atoms exceeds $\pm 1\%$ of E_c . The energy is averaged over all atoms located in a plane parallel to GB. Note, cohesive energy in the bulk, which is given by EAM potential, is -4.122 eV. The example of the assessment of GB $\Sigma 17(410)$ width is shown in Fig. 2. This parameter

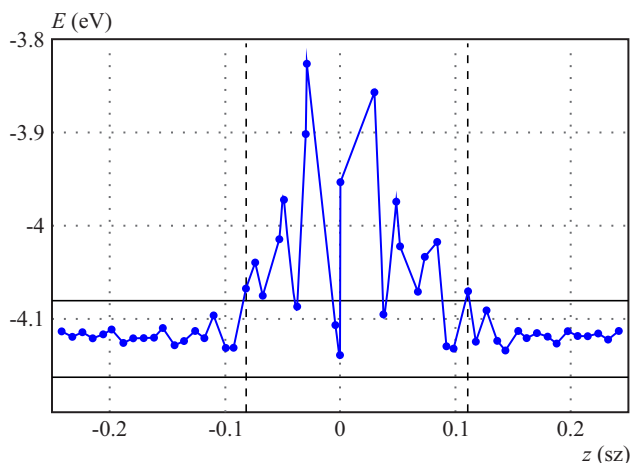


Fig. 2. The width of GB $\Sigma 17(410)$ is indicated by dashed lines. The width is set as an area where average energy of atoms located in a plane (410) exceeds $\pm 1\%$ of cohesive energy. Coordinate in z -direction is related to the cell dimension (sz).

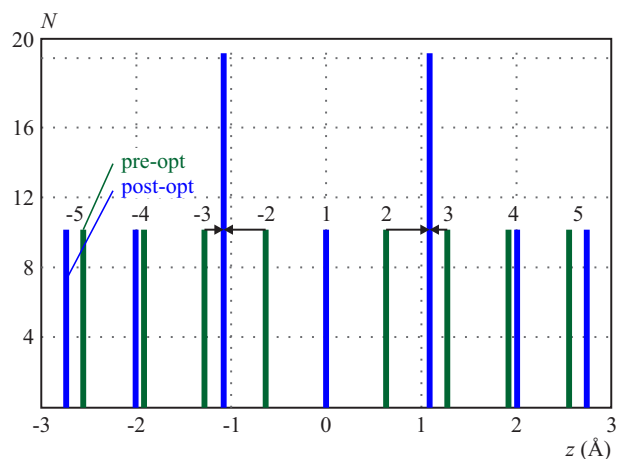


Fig. 3. Dependence of number of atoms within plane (210) as a function of plane position in z -direction for GB $\Sigma 5(210)$ before optimization (orange bars) and after optimization (black bars). GB is placed at $z = 0$. Planes are labeled by numbers. Plane relaxation is outlined by arrows.

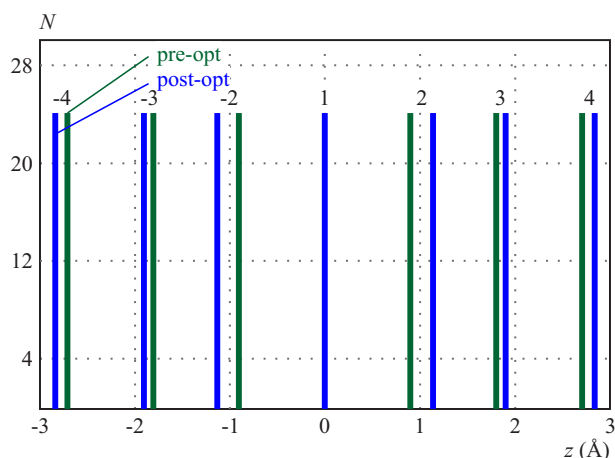


Fig. 4. Dependence of number of atoms within plane (310) as a function of plane position in z -direction for GB $\Sigma 5(310)$ before optimization (orange bars) and after optimization (black bars). GB is placed at $z = 0$. Planes are labeled by numbers.

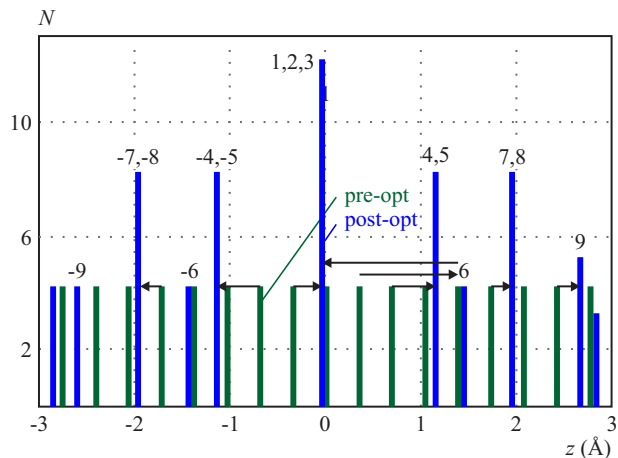


Fig. 5. Dependence of number of atoms within plane (410) as a function of plane position in z -direction for GB $\Sigma 17(410)$ before optimization (orange bars) and after optimization (black bars). GB is placed at $z = 0$. Planes are labeled by numbers. Plane labels correspond to atomic labels in Fig. 7. Atomic relaxation in z -direction is outlined by arrows.

gives valuable information for investigation of impurity and defect segregation on GBs.

3 DISCUSSION

Number of atoms within a plane parallel to GB as a function of plane position in z -direction before and after optimization is shown in Figures 3 to 6 for GBs $\Sigma 5(210)$, $\Sigma 5(310)$, $\Sigma 17(410)$ and $\Sigma 13(510)$, respectively. These figures demonstrate change of inter-planar distances as well as change of atomic density within planes parallel to GB. The width of the window where atoms were considered as lying in one plane was set to 0.23 \AA . The GB $\Sigma 5(210)$ (see Fig. 3) doubled the atomic density in the planes adjacent to the boundary. This phenomenon can be easily explained by an outward relaxation of planes

$-2, 2$ and inward relaxation of planes $-3, 3$. The shift of inter-planar distances between planes (210) and (310) was identified as the main process of relaxation for GBs $\Sigma 5(210)$ and $\Sigma 5(310)$ (see Fig. 3 and 4). Moreover, for GB $\Sigma 5(210)$ the mechanism was complemented by a rigid shift of one grain with respect to another one in x -direction. Note, the shift was 16.8% of the lattice parameter. In case of the remaining two interfaces $\Sigma 17(410)$ and $\Sigma 13(510)$ optimization process looks much more complicated (see Fig. 5) because those interfaces undergo reconstruction. A common feature of the reconstruction process is that the density of atoms located in GB plane increases which is in contrast with the relaxation process of GB $\Sigma 5(310)$. This can be in fact seen in Fig. 5 as well as in Fig. 6 and, for comparison, in Fig. 4. The increase of the atomic density within $\Sigma 17(410)$ and $\Sigma 13(510)$ GB planes is definitely not a consequence of the inward and

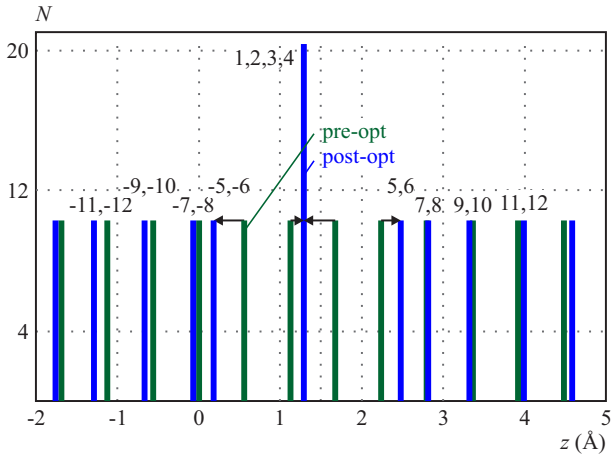


Fig. 6. Dependence of number of atoms within plane (510) as a function of plane position in z -direction for GB $\Sigma 13(510)$ before optimization (orange bars) and after optimization (black bars). Initial GB is placed at $z = 0$, optimized GB is placed at $z = 1.29 \text{ \AA}$. Planes are labeled by numbers. Plane labels correspond to atomic labels in Fig. 8. Atomic relaxation in z -direction is outlined by arrows.

Table 2. Atomic density of GB plane (σ_{GB}) and atomic density of parallel plane in bulk (σ_{bulk}). Width (w) of α -iron $\langle 100 \rangle$ symmetric tilt grain boundaries featured in both, absolute value and relative value related to the lattice parameter (a)

GB	$\sigma_{GB} (\text{\AA}^{-2})$	$\sigma_{bulk} (\text{\AA}^{-2})$	$\sigma_{GB} / \sigma_{bulk}$	$w (\text{\AA})$	w/a
$\Sigma 5(210)$	0.0549	0.0549	1	5.48	2.0
$\Sigma 5(310)$	0.0776	0.0776	1	5.68	2.0
$\Sigma 17(410)$	0.0893	0.0298	3	7.46	2.6
$\Sigma 13(510)$	0.0962	0.0481	2	7.42	2.6

Table 3. Grain boundary energy of α -iron $\langle 100 \rangle$ symmetric tilt grain boundaries

$E_{GB} (\text{Jm}^{-2})$	Terentyev[8]	Tschopp[9]	our work
$\Sigma 5(210)$	1.3925	1.096	1.462
$\Sigma 5(310)$	0.9853	0.987	1.053
$\Sigma 17(410)$	1.1123	-	1.231
$\Sigma 13(510)$	1.8432	0.992	1.070

outward atomic plane relaxation as in the case of GB $\Sigma 5(210)$. It can be achieved only by concurrent migration of atoms between planes parallel and perpendicular to interface. The process of the reconstruction in detail is shown in Figs. 7 and 8 for GBs $\Sigma 17(410)$ and $\Sigma 13(510)$, respectively.

A detailed description of the reconstruction process for GB $\Sigma 17(410)$ looks as follows: before the optimization process (see Fig. 7a), atom 3 is positioned in plane (001) and its twin across the GB, atom -6 , is also positioned in plane (001). During the optimization process, atom 3 migrates to the position in GB plane (see Fig. 7b). This migration requires, from the energetic reasons, migration of the atom to the plane (002). Consequently, atom 6 which was initially positioned unrealistic close to atom 2

migrates from plane (002) into plane (001) occupying original position of the atom 3. This atomic transfer can occur also from other side of GB plane including atoms 2, -6 instead of atoms 6, 3. In the case of GB $\Sigma 13(510)$, see Fig. 6, we could claim that increased atomic density on GB plane was achieved by the same process of the inward and outward atomic plane relaxation as in the case of GB $\Sigma 5(210)$. Actually, the optimization process was much more complicated (see Fig. 8). At the beginning (see Fig. 8a), the interface is located along the line determined by positions of the atoms -8 and -7 . After completion of the optimization process (see Fig. b), the interface changes position and is located along line determined by positions of the atoms 1 and 2. As a consequence, atoms -5 and -6 can pass into open space defined by triplets of atoms 1, -12 , -9 and 2, -11 , 10. Atoms 3 and 4 move to GB plane where the atomic density is consequently increased. This quite complex transfer of atoms in the vicinity of the interface is possible due to the transition of atoms between planes (001) and (002). As a consequence of this atomic transfer, GB plane changes its position from $z = 0$ to $z = 1.29 \text{ \AA}$.

Atomic densities of GB planes after optimization compared with atomic densities of parallel planes in bulk are summarized in Table 2. This parameter, besides the atomic transfer process presented in Figures 7 and 8, supports the idea of GB reconstruction, while increased atomic density of GB plane indicates a change of the interface topology. GBs $\Sigma 17(410)$ and $\Sigma 13(510)$ are characterized by 3- and 2-times increased atomic density of GB plane and consequently can be identified as reconstructed. Moreover, we found that the GB width values may decide whether the structure relaxes or undergoes reconstruction. The values are summarized in Tab. 2. Calculated data indicate that the width of the relaxed structure is shorter (specifically 2-times lattice parameter) than the width of the structure after reconstruction (specifically 2.6-times lattice parameter). This in fact indicates that relaxed GBs affect closer region around the interface compared to the width of reconstructed GBs. The weakest effect of spreading disorder to the surrounding area was observed in the case of GB $\Sigma 5(310)$. On the other hand, the most significant effect on the interface width was observed in the case of GB $\Sigma 17(410)$. These observations are in good agreement with the results recently published in [8].

Computed energies of investigated GBs are summarized and compared with results obtained by Terentyev et al. [8] and Tschopp *et al* [9] in Table 3. It should be noted that both authors used the same EAM potential parametrization as in our simulation. Nevertheless, optimization methods applied in [8, 9] differ from methods applied in our simulation. The applied optimization methods are: quenching within molecular dynamics (MD) [8], MD combined with non-linear conjugate gradient algorithm [9] and simulated annealing combined with genetic algorithm (our work). However, there is a large discrepancy between ours and Terentyev's result for GB

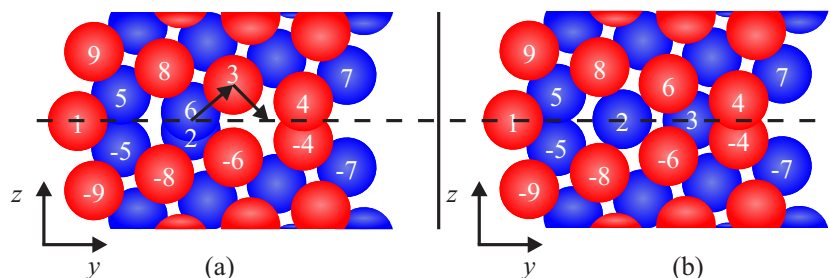


Fig. 7. Structure of GB $\Sigma 17(410)$ (a) — before and (b) — after optimization. Red and blue color represents atoms in plane (001) and (002), respectively. Arrows indicate atomic migration.

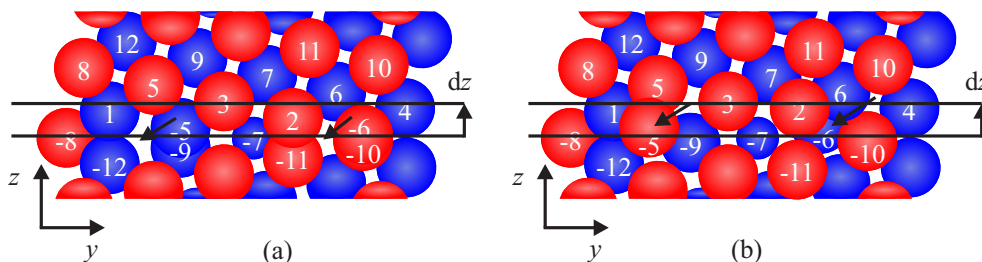


Fig. 8. Structure of GB $\Sigma 13(510)$ (a) — before and (b) — after optimization. Red and blue color represents atoms in plane (001) and (002), respectively. Arrows indicate atomic migration. GB plane migration is indicated by dz .

$\Sigma 13(510)$ and between ours and Tschopp's result for GB $\Sigma 5(210)$. We believe that differences are due to the application of different optimization methods. Note, when the reconstruction of the $\Sigma 13(510)$ interface was forbidden, which effectively means that the migration of atoms between planes (001) and (002) was not allowed, the resulting GB energy was unacceptably high (about 2 Jm^{-2}). It is exactly the case reported in Ref. [8]. In the case of GB $\Sigma 5(210)$, it can be seen that the energy obtained by Tschopp was 1.096 Jm^{-2} , which is less than the energy achieved in our simulation. The structure, in which the resulting energy 1.096 Jm^{-2} was reached, comprises at GB atoms in plane (001) and also in plane (002). The same structure was presented also in first-principles calculation [12]. In contrast, the structure obtained by our simulation contains at GB only one atom positioned in plane (001). The most probable explanation is that configuration presented in [9, 12] corresponds to our configuration with vacancy at GB. If one atom is removed from our configuration, the GB energy decreases to 1.128 Jm^{-2} , which is energy nearby Tschopp's value 1.096 Jm^{-2} . Despite the fact that ours and Terentyev's result for GB $\Sigma 17(410)$ is in very good agreement, optimized structures are different. Unlike the Terentyev simulation that confirmed the shift of grains toward each other in y -direction, our result revealed reconstruction.

4 CONCLUSION

We have investigated the process of relaxation/reconstruction of four α -iron $\langle 100 \rangle$ symmetric tilt grain boundaries: $\Sigma 5(210)$, $\Sigma 5(310)$, $\Sigma 17(410)$ and $\Sigma 13(510)$.

We have analysed atomic plane distribution in the direction perpendicular to GB plane as well as atomic rearrangement within GB plane.

It has been shown that prominent feature of some GBs is the ability to reconstruct a structure during optimization process, which in fact reduces the final energy. The effect of reconstruction was observed at GBs $\Sigma 17(410)$ and $\Sigma 13(510)$. It was accompanied by significant reduction in energy to 1.23 Jm^{-2} and 1.07 Jm^{-2} . Reconstruction was allowed by concurrent migration of some atoms in the direction parallel and perpendicular to GB plane. The migration of atoms invokes the increase of the atomic density in GB plane and consequently changes topology of the interface. The most stable structure associated with only a small movement of atoms and lowest GB energy 1.05 Jm^{-2} is GB $\Sigma 5(310)$. On the other hand, as the least stable structure was identified GB $\Sigma 5(210)$ with the energy of 1.46 Jm^{-2} , despite the fact that during the relaxation process atoms made a fairly large shift in the vicinity of the interface. From energetic point of view, the region influenced by reconstructed GBs is about 30% wider than region influenced by relaxed GBs.

REFERENCES

- [1] MALERBA, L.—CARO, A.—WALLENIUS, J.: Multiscale Modelling of Radiation Damage and Phase Transformations: The Challenge of FeCr Alloys, *J. Nucl. Mater.* **382** (2008), 112–125.
- [2] SUGINO, Y.—UKAI, S.—LENG, B.—OONO, N.—HAYASHI, S.—KAITO, T.—OHTSUKA, S.: Grain Boundary Related Deformation in ODS Ferritic Steel During Creep Test, *Mater. Trans.* **53** No. 10 (2012), 1753–1757.
- [3] STECKMEYER, A.—RODRIGO, V. H.—GENTZBITTEL, J. M.—RABEAU, V.—FOURNIER, B.: Tensile Anisotropy and

- Creep Properties of a Fe–14CrWTi ODS Ferritic Steel, *J. Nucl. Mater.* **426** (2012), 182–188.
- [4] MISHIN, Y.—ASTA, M.—LI, J.: Atomistic Modelling of Interfaces and their Impact on Microstructure and Properties, *Acta Mater.* **58** No. 148 (2010), 1117–1151.
- [5] RACE, C. P.—HADIAN, R.—von PEZOLD, J.—GRABOWSKI, B.—NEUGEBAUER, J.: Mechanisms and Kinetics of the Migration of Grain Boundaries Containing Extended Defects, *Phys. Rev. B* **92** (2015), 174115.
- [6] COMBE, N.—MOMPIOU, F.—LEGROS, M.: Disconnections Kinks and Competing Modes in Shear-Coupled Grain Boundary Migration, *Phys. Rev. B* **93** (2016), 024109.
- [7] IBACH, H.: *Physics of Surfaces and Interfaces*, Springer-Verlag, Berlin, Heidelberg, 2006.
- [8] TERENCEV, D.—HE, X.: Properties of Grain Boundaries in bcc Iron and Iron-Based Alloys, SCK•CEN, Mol, Belgium, no. BLG-1072, 2010.
- [9] TSCHOPP, M. A.—SOLANKI, K. N.—GAO, F.—SUN, X.—KHALEEL, M. A.—HORSTEMEYER, M. F.: Probing Grain Boundary Sink Strength at the Nanoscale: Energetics and Length Scales of Vacancy and Interstitial Absorption by Grain Boundaries in α -Fe, *Phys. Rev. B* **85** (2012), 064108.
- [10] DAW, M. S.—BASKES, M. I.: Embedded-Atom Method: Derivation and Application to Impurities, Surfaces, and other Defects in Metals, *Phys. Rev. B* **29** No. 12 (1984), 6443–6453.
- [11] MENDELEV, M. I.—HAN, S.—SROLOVITZ, D. J.—ACKLAND, G. J.—SUN, D.—ASTA, M.: Development of New Interatomic Potentials Appropriate for Crystalline and Liquid Iron, *Philos. Mag.* **83** (2003), 3977–3994.
- [12] WU, M.—GU, J.—JIN, Z.: Migration Energy Barriers of Symmetric Tilt Grain Boundaries in Body-Centered Cubic Metal Fe, *Scripta Mater.* **107** (2015), 75–78.

Received 3 August 2016

Eva Vitkovská (Ing) was born on 6-th September 1987 in Žilina. She graduated from the Faculty of Electrical Engineering and Information Technology, Slovak University of Technology in Bratislava, in 2012. Subsequently, she has started PhD. degree in Physical Engineering at Faculty of Electrical Engineering and Information Technology, Slovak University of Technology in Bratislava. Research experience gained abroad: Summer 2014, Paul Scherrer Institute, Switzerland Her research experience and interest include: solid state physics, parallel computing, optimization techniques, first principles calculations, grain boundary structure, mechanical and magnetic properties of iron grain boundaries, simulation of positron lifetime in uranium dioxide.

Peter Ballo (Prof, Ing, PhD) graduated from the Faculty of Electrical Engineering, Slovak University of Technology, Bratislava, in 1984, and received his CSc. (PhD.) degree in Solid State Physics in 1993. He joined the Department of Physics at the Faculty of Electrical Engineering, Slovak University of Technology, Bratislava, as an Assistant (1989), Associate Professor (1996) and Full Professor (2008). Research experience gained abroad: 1987-1988 Joint Institute for Nuclear Research, JINR, the Russian Federation, 1992-1994 University Siegen, Germany, 1997 Forschungszentrum Karlsruhe, Germany, 1997-2000 California State University, Northridge, California, USA. His research experience and interest include: numerical modelling and simulation, parallel computing, theory and applications in classical electrodynamics, nonlinear systems and spin-dependent effects. The results were published in more than 150 publications (more than 40 papers were published in CC scientific periodicals or as chapters in books).